SERS Analysis of CMC on Gold-Assembled Micelle

Nak Han Jang

Institute of Science Education, Kongju National University, Kongju, Chungnam 314-701, Korea
Received June 25, 2004

The micellization of dodecylpyridinum chloride (DPC) assembled on aqueous gold nanoparticles has been studied as a function of concentration using Surface-Enhanced Raman Scattering (SERS). At the low concentration, the strong SERS band of the benzene ring moiety was observed at 1025 cm^{-1}, and assigned to "trigonal ring breathing". According to high concentration of DPC, a new strong band was also appeared at 1012 cm^{-1}, which was assigned to "totally symmetry ring breathing". The difference of two spectra seems to ascribe to the geometry of polar head group, *i.e.*, pyridinium cation. These geometry exist flat-down at low concentration, whereas standing-up or tilted geometry at high concentration. The critical micelle concentration (CMC) was first obtained from the ratio of intensities of the two bands related to the benzene ring moiety by vibrational spectroscopy, and was about 28 mM. After the CMC, the benzene ring moiety in the micelle state was more restricted than in monomer state because there is no more change of intensities at 1012 cm^{-1}. In addition, the size of gold-assembled micelle was estimated using light scattering and it was about 328.3 nm.

Key Words : SERS, Cationic surfactant, CMC, Gold nanoparticles

Introduction

Surface-Enhanced Raman Scattering (SERS) is a very versatile technique to obtain the powerful information of characterizing the absorption and orientation of adsorbate on molecule-surface interactions.[1,2] The SERS is a process in which the Raman scattering intensity of molecules adsorbed on certain rough metal surface, (*e.g.*, Ag, Au, Cu) is enhanced by factors of 10^4-10^6 compared to the intensity expected for unadsored molecules of a comparable concentration.[3,4] This enormous sensitivity enhancement easily allowed adsorbates of a submonolayer coverage to be readily detected by Raman spectroscopy.

Although not all molecules show enhancement at each interface, molecules which typically show enhancement at the solution-solid interface have unshared pairs of electrons, *e.g.* pyridine, piperidine and CN^-. Some important contradictions were attributed to a SERS spectrum for pyridinium ion which has unshared pair of electrons and the lack of a SERS spectrum of pyridine at low pH due to formation of pyridinium ion on silver surface.[4,5] However, because the pyridinium ion may not be able to adsorb on the surface itself, the SERS spectrum of pyridinium ion can be observed only when anion is present may be a consequence of greater enhancement due to anion.[6] The anion has a much greater affinity for the surface and is more polarizable. The anion also interacts strongly with the pyridinium cation. The affinity of anion for both the metal and the pyridinium ion may produce greater molecule-metal coupling. Thus, the enhancement may arise from a surface species of metal-anion-pyridinium cation. Here, in cationic surfactant, dodecylpyridinum chloride (DPC), there is no unshared pair of electrons on the nitrogen, as there is in pyridine, and thus there is little interaction with the gold surface. However, because pyridinium cation also adsorb more strongly to Cl^-, the SERS spectrum is observed, indicating an enhanced coupling between the pyridinium cation and the gold surface *via* an adsorbed Cl^- complex.

Cationic surfactants are amphiphilic molecules that contain a hydrophobic (nonpolar) alkyl chain, commonly called "the tail", and a hydrophilic (polar) cation segment, called "the head". This characteristic of being an amphiphilic molecule leads to aggregation. They reduce the surface tension by forming an extremely small aggregate that is called micelles. At low concentrations, surfactants are soluble in water, and increasing their concentration, the molecules of surfactants form micelles in solution. The smaller concentration at which micelles begin to form is called as the Critical Micelle Concentration (CMC).[7,8] Because micelles is consisted of polar head groups on each opposing surface with hydrophobic material in molecule, they are a form of a continuous bilayer of surfactant molecules. In other words, at or near the CMC micelles form in solution and bilayers form on surfaces. Until now, various methods are reported to determine the CMC of micelle on cationic surfactant using fluorescence,[9] electrical conductivity,[9] light scattering,[10] density,[11] viscosity,[11] ultrasonic relaxation,[12] and NMR[13] but is not reported any method to use vibrational spectroscopy.

In this paper, the method to characterize the CMC of micellization is first reported on gold nanoparticles-assembled cationic surfactant using Raman spectroscopy and is elucidated the orientation of pyridinium moiety with a comparative analysis during micellization. In addition, the bulk size of gold-assembled micelle is proposed using the particle analyzer.

*e-mail: nhjang@kongju.ac.kr

Experimental Section

Materials: Dodecypyridinium chloride (DPC) was of analytical quality and was purchased from Aldrich Chemical Company and used without any more purification. All solutions were prepared from the stock solution. For all experiments, purified H_2O (18.1 MΩ) was used and all glassware was cleaned in aqua regia (3 parts HCl, 1 parts HNO_3). Approximately 13 nm diameter gold particles were prepared by the citrate reduction of $HAuCl_4$ as described previously.[14] Stock solutions for DPC were prepared from 10^{-3} M to 5×10^{-1} M concentration. The adsorbate was introduced in 1 mL gold nanoparticles by adding one drop (about 0.025 mL) by drop of the above stock solutions, which resulted in a change of solution color from deep red to blue. A few drop of 3% poly(vinylpyrrolidone) (PVP, MW 10000) was added to the sample as a stabilizer, preventing further aggregation and eventual flocculation of the nanoparticle. The overall concentration of each DPC was from about 2.5×10^{-5} M to 5.0×10^{-2} M in surfactant/Au sample.

UV Spectra and Micelle Size: UV-Visible spectra were recorded on a Hewlett-Packard 8452A diode array spectrophotometer. A typical solution of 13 nm diameter gold particles exhibited a characteristic surface plasmon absorption maximum at 520 nm. After modifying with DPC, the aggregation of particles is also monitored by UV-Visible spectroscopy. Dynamic Light Scattering measurements were performed to characterize the size of gold-assembled micelle using a Brookhaven Instruments Corporation model BI-9000AT digital autocorrelator and photon counter with a model BI-200SM goniometer. Incident light was provided by an argon ion laser (λ_{ex} = 514.5 nm) operating at 300 mW (Lexel Corp). Scattered light was collected at a fixed angle of 90°. The DPC-linked gold nanoparticle aggregate samples were prepared as described above. The gold-assembled micelles were filtered through a 0.22 μm acetate membrane filter prior to mixing to remove any dust particles.

Raman Spectroscopy: The Raman spectra were taken as described previously.[14] Raman spectrum of solid sample were achieved by using FT-Raman spectrometer (BioRad) equipped with 1064 nm Nd:YAG laser(Spectra Physics). For the SERS spectra, the Ar^+ laser was used to pump a Spectra Physics Tsunami model locked Ti:Al_2O_3 laser to obtain λ_{ex} = 710 nm. A band pass filter (Oriel Corporation, Stratford, CT) centered at 710 nm with a 10 nm range was utilized for removing extra lines. Spectra were recorded at λ_{ex} = 710 nm using a SPEX Model 1877 Triplemate triple grating monochromator, and a SPEX Spectrum One charge-coupled device (CCD) detector.

Results and Discussion

The processes of adsorption on DPC and micellization on gold-based DPC were proposed in Figure 1. Basically, DPC is a cationic surfactant and it cannot directly adsorb to gold surface because pyridinium cation has no unshared pair of electrons. However, Cl^- has a much greater affinity for the gold surface and directly adsorb on the gold surface. Cl^- also interacts strongly with the pyridinium cation. Consequently, the affinity of Cl^- for both the gold and the pyridinium cation produce greater molecule-metal coupling to enhance the SERS effect and the DPC spectrum is observed, indicating an enhanced coupling between the pyridinium cation and the gold surface *via* an adsorbed Cl^- complex. After the DPC monolayer adsorbs to gold surface, the DPC-based gold nanoparticle is aggregating hugely, shifting the red to blue

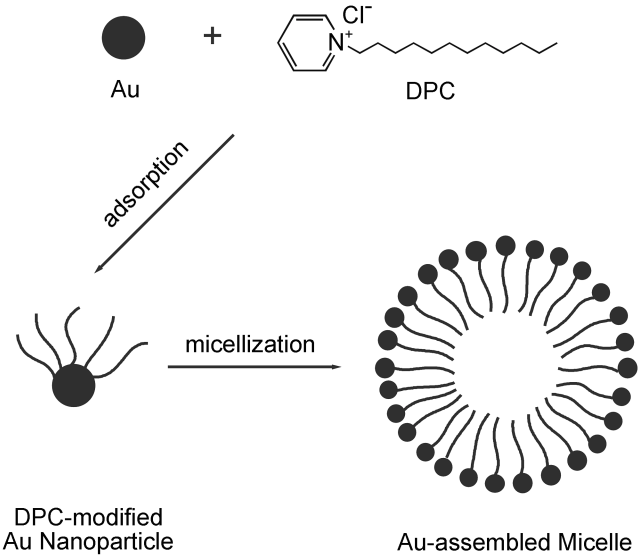

Figure 1. Schematic diagram of micellization on gold nanoparicle-based DPC.

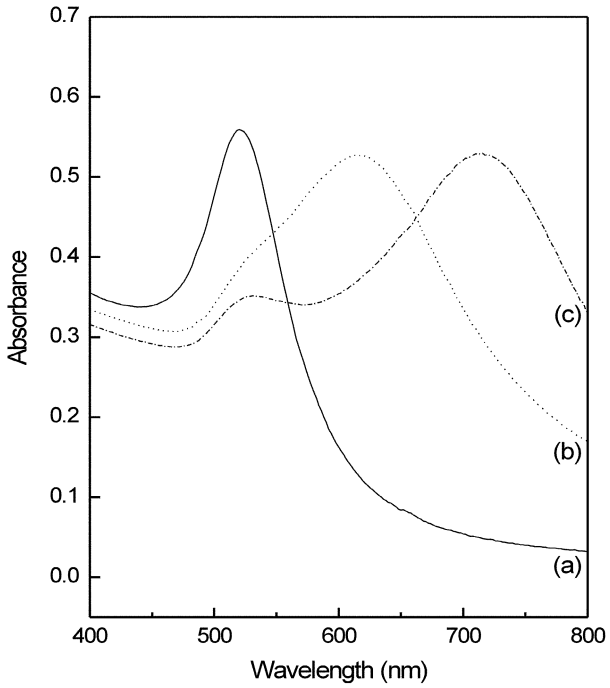

Figure 2. Plots of UV-Visible absorption spectra of gold nanoparticles: (a) in the absence of DPC (the solid line), (b) 5 minutes after modifying with 1×10^{-4} M DPC (dotted line), and (c) 5×10^{-2} M DPC (the dash-dotted line).

color. The UV-Visible absorption spectra were used to monitor the binding affinity of DPC to 13 nm diameter gold nanoparticles in Figure 2. The UV-Visible spectrum (spectrum a) of 13 nm diameter gold nanoparticles is shown for reference, which has a maximum at about 520 nm in Figure 2(a). Figures 2(b) and 2(c) show the changes in the plasmon band when DPC was added to a solution of 13 nm diameter gold nanoparicles, 1×10^{-2} M and 5×10^{-2} M DPC, respectively. To prevent further aggregation and eventual flocculation of the gold nanoparticles, the stabilizer was added in drop by drop and samples were waited for five minutes. At the low concentration (b) below CMC, all of DPC monolayer exhibited major changes in the maximum plasmon region at 615 nm. Furthermore, at a high concentration (c) over CMC, the gold-based DPC was micellized and showed major changes in the maximum plasmon region at 716 nm. This state of aggregation was stable existing further no more change for an hour.

Figure 3 shows the Raman spectra of pyridine and DPC at several states. The Raman spectra of pyridine were introduced to compare with the main peak of DPC because it bears the pyridinium ring structure in the head chain. Assignments of Raman band frequencies for DPC were determined by comparing the frequencies of the observed Raman data with the vibrational data of references.[15,16] These tentatively assignments for SERS bands are listed in Table 1 for comparison the measured normal and FT-Raman frequencies in solution and in the solid. In Figure 3(g), the SERS band at 1012 cm^{-1} is due to the ring-breathing mode (Wilson mode 1 of benzene ring) of DPC adsorbed on gold nanoparticle surface, which is from mono-substituted benzene mode. This band is compared to the band (ring-breathing mode) at 998 cm^{-1} of pyridine adsorbed on gold nanoparticle surface in Figure 3(b). In Figure 3(e), this band is also not observed in the low DPC concentration. When DPC is dissolved at low concentrations, the molecules exist as individual entities. It is tentatively proposed a flat-on arrangement of DPC that the benzene ring moiety is parallel to the gold surface. That is, DPC is lying down on the surface because of the hydrophobic alkyl chain. Depending on the function of DPC concentration, this band is increased up to the maximum. This phenomenon can be supposed by the change of environment in pyridinium cation on the gold surface. At a high concentration of DPC, the pyridinium cation adsorbs on perpendicular to the gold surface, meaning that the benzene ring moiety is standing up to the gold surface. Increasing the concentration of DPC, the hydrophobic effect is also increased by the alkyl chain and the micelle is formed to reduce the hydrophobicity. Consequently, DPC is restricted by gold nanoparticles and the benzene ring moiety of pyridinium cation has to stand up to the gold surface. The band at 1025 cm^{-1} corresponds to the trigonal ring-breathing mode (Wilson mode 12 of benzene ring) of DPC adsorbed on gold surface. This band is typically appearing at the ring of benzene derivatives. The position of this band is in a good agreement with the adsorption of neutral pyridine on gold nanoparticle surface and the result

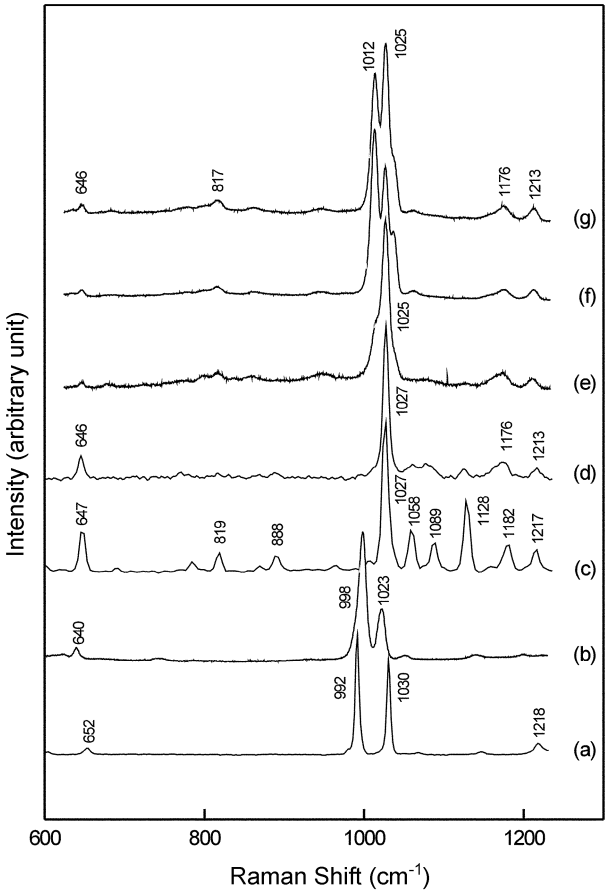

Figure 3. Comparison of pyridine and DPC Raman spectra: (a) FT-Raman spectrum of pure pyridine. (b) SERS spectrum of 1×10^{-3} M pyridine on gold nanoparticles. (c) FT-Raman spectrum of solid DPC. (d) 5×10^{-1} M DPC in aqueous solution. (e) SERS spectrum of 1×10^{-5} M. (f) 2.5×10^{-2} M DPC (g) 5×10^{-2} M DPC on gold nanoparticles.

Table 1. Assignments of Raman spectra for DPC

Pyridine		DPC			Tentative Assignment
Liquid	SERS	Solid	Aqueous	SERS	
652	640	647	646	646	Ring Deformation
		819		817	Ring Vibration
992	998			1012	Ring Breathing
1030	1023	1027	1027	1025	Trigonal Ring Breathing
		1182	1176	1176	C-C stretching
1218		1217	1213	1213	Ring-C vibration

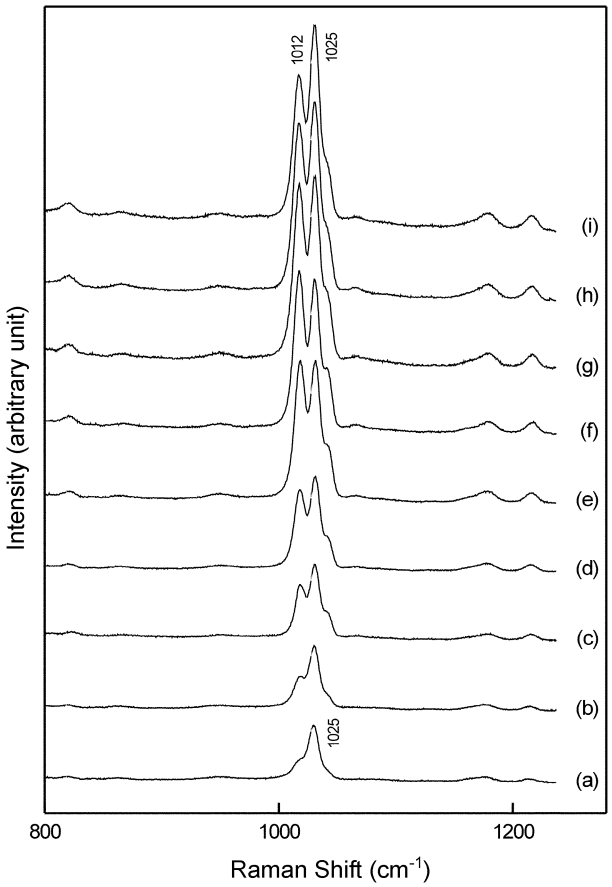

Figure 4. SERS spectra of DPC as a function of concentration: (a) 2.5×10^{-5} M (b) 1.25×10^{-4} M (c) 1.0×10^{-3} M (d) 5.0×10^{-3} M (e) 1.0×10^{-2} M (f) 2.0×10^{-2} M (g) 3.0×10^{-2} M (h) 4.0×10^{-2} M (i) 5.0×10^{-2} M. All spectra were normalized by the reference (a). For clarity of presentation, spectra were offset, respectively.

reported in previous SERS work.[17]

As the concentration of the DPC increases the molecules tend to associate to form aggregates. In aqueous solutions, the hydrophobic tails of the DPC associate, leaving the (hydrophilic) headgroups exposed to the solvent. Therefore, the environment of benzene ring moiety is different from the function of DPC concentration. The SERS spectra of benzene ring moiety are displayed as the function of DPC concentration in Figure 4. As is mentioned before, there is no band at 1012 cm^{-1} at very low DPC concentration because the benzene ring moiety is parallel to the surface. However, this band increases up because the benzene ring moiety is standing up to the surface as the concentration of DPC increases. After the CMC, the intensities of this band do not change although the concentration increases further. This reason is why once the micelles are formed, further increase of the total DPC concentration does not change the concentration of gold-assembled molecules on micelle. The DPC added is completely incorporated into the micelles without any assembly with gold nanoparticles. In other words, the concentration of the gold-assembled DPC molecules remains constant after the micelles are formed. After the CMC, the intensities of band at 1025 cm^{-1} are

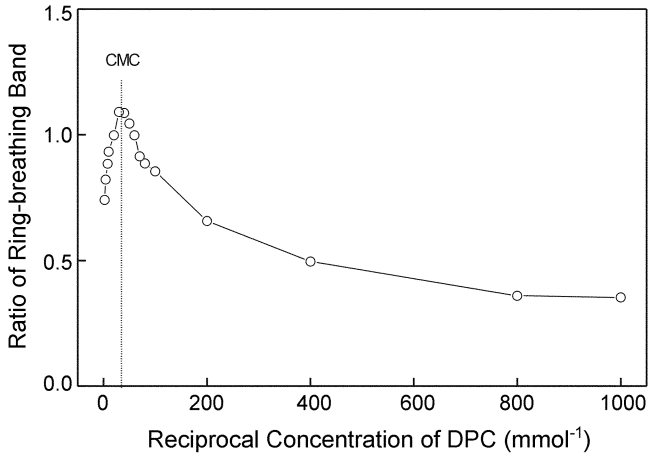

Figure 5. The ratio of ring breathing band intensities (1012 cm^{-1}/ 1025 cm^{-1}) as a function of concentration. After the baseline is referred near 950 cm^{-1}, each of intensity is subtracted by the baseline.

increased higher than that of the band at 1012 cm^{-1}. Because the ratio of relative intensity changes between 1012 cm^{-1} and 1025 cm^{-1} related to the benzene ring moiety of DPC, the transition from a monomeric solution to a micelle form can be seen as a change in the slope of plots against DPC concentration of the ratio of relative intensity related to the benzene ring moiety. Here the new method was proposed to determine the CMC of gold assembled micelle using SERS. Figure 5 was plotted against the reciprocal concentration of DPC to the ratio of relative intensities between 1012 cm^{-1} and 1025 cm^{-1}. The slope is changing before and after the CMC. Therefore, the CMC is determined at the maximum which shows the inversion of sign in slope. In the result, the CMC was about 28 mM on gold-assembled DPC micelle. This value is pretty larger than the CMC (17 mM) of pure DPC micelle reported[11,18] because DPC is assembled with the 13 nm gold nanoparticle. This study first shows the possibility of determination of CMC by vibrational spectroscopy. In addition, this method is valuable for the other CMC which is very small because SERS is very sensitive.

Finally, the size of gold-assembled micelle was estimated using light scattering because typically the micelles have a closely spherical shape in a rather wide concentration range above the CMC (Figure 6). The size of gold-assembled micelle was about 328.3 nm from multimodal size distribution during the average of four runs. This size is pretty huge compared with the size (50 nm) estimated from the general alkyl chain micelle.[7] This reason can be considered as the aggregation of gold particle and the repulsion of positive charge because Cl^- is first tethered to the gold surface to adsorb the pyridinium cation. In formation of the pure micelle, the small amount of added NaCl decreases the CMC of DPC.[18] This is due to the decrease in the electrical repulsion between the positively charged head groups in the micelle in the electrolyte solution. The effect of added NaCl on the CMC is much pronounced for the high hydrophobicity. Here the concentration of Cl^- reduces in gold-based DPC because chloride anion has a much greater

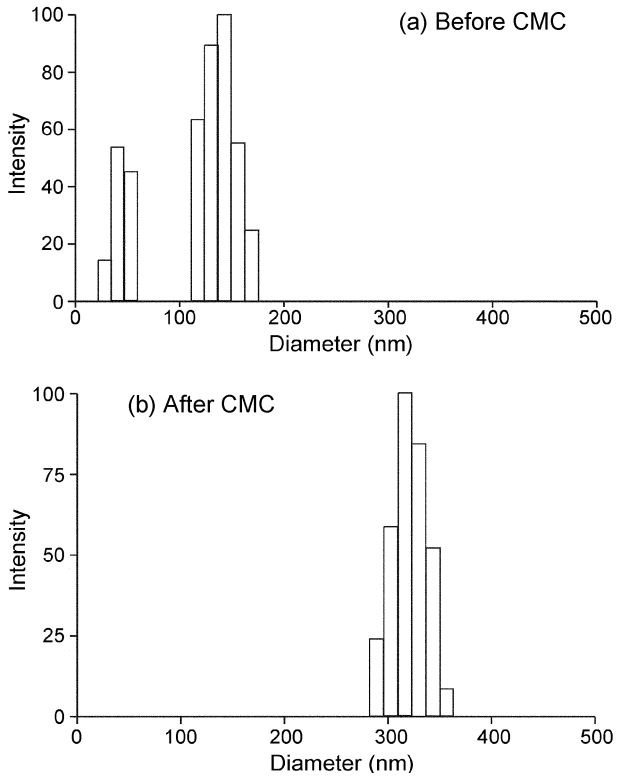

Figure 6. Multimodal size distribution of DPC-assembled micelle measured by light scattering: (a) Before CMC (b) After CMC. Effective Diameter: 328.3 nm, Polydispersity: 0.121, Sample Quality: 7.3.

affinity for the gold surface and the hydrophobicity also reduces because the gold-based DPC is increasing the hydrophilicity. Moreover, the repulsion of positively charged head groups increases as the concentration of DPC increases. Consequently, more aggregation number need to form the micelle and this induces to increase the size of gold-assembled micelle.

Conclusions

Good-quality SERS spectra of DPC were first acquired on gold nanoparticles and the CMC of gold-assembled micelle was determined although it is well-known to difficulty of the cationic surfactant on SERS because it cannot adsorb to the surface. Because the Cl^- has a much greater affinity for the gold surface and it also interacts strongly with pyridinium cation, it would be observed the SERS spectra of DPC on gold nanoparticles. At the low DPC concentration, the SERS band at 1025 cm^{-1} was only predominant, which was related to the benzene ring moiety, assigned to "trigonal ring breathing". Increasing the concentration of DPC, a new strong band was strongly appeared at 1012 cm^{-1}, which was assigned to "totally symmetry ring breathing". This difference seems to ascribe to the geometry of polar head group, *i.e.*, pyridinium cation. These geometry exist flat-down at low concentration, whereas standing-up or tilted geometry at high concentration. The critical micelle concentration (CMC) was first obtained from the ratio of intensities of the two bands (1012 cm^{-1}/1025 cm^{-1}) related to the benzene ring moiety by vibrational spectroscopy, and was about 28 mM. After the CMC, the benzene ring moiety in the micelle state was more restricted than in monomer state because there is no more change of intensities at 1012 cm^{-1}. In addition, the size of gold-assembled micelle was determined using light scattering and it was about 328.3 nm. The large size of gold-assembled micelle is due to the decrease in the electrical repulsion between the positively charged head groups in the micelle

Acknowledgment. Author thanks for the partially financial support of Korean Research Foundation (KRF-2003-005-C00033) and also expresses his deepest appreciation to Professor Mirkin at Northwestern University.

References

1. (a) Koglin, E.; Séquaris, J. M.; Valenta, P. *J. Mol. Struct.* **1980**, *60*, 421-425. (b) Ervin, K. M.; Koglin, E.; Séquaris, J. M.; Valenta, P.; Nürnberg, H. W. *J. Electroanal. Chem.* **1980**, *114*, 179-194. (c) Creighton, J. A. *Surf. Sci.* **1985**, *158*, 211-221.
2. (a) Angebranndt, M. J.; Winefordner, J. D. *Talanta* **1992**, *39*, 569-572. (b) Jordan, C. E.; Frutos, A. G.; Thiel, A. J.; Corn, R. M. *Anal. Chem.* **1997**, *69*, 4939-4947. (c) Angel, S. M.; Katz, L. F.; Archibald, D. D.; Honigs, D. E. *Appl. Spectrosc.* **1989**, *43*, 367-372. (d) Pate, J.; Leiden, A.; Bozlee, B. J.; Garrell, R. L. *J. Raman Spectrosc.* **1991**, *22*, 477-480. (e) Szafranski, C. A.; Tanner, W.; Laibinis, P. E.; Garrell, R. L. *Langmuir* **1998**, *14*, 3570-3579.
3. Fleischmann, M.; Hendra, P. J.; McQuillan, A. *Chem. Phys. Lett.* **1974**, *26*, 163-166.
4. Jeanmarie, D. L.; Van Duyne, R. P. *J. Electroanal. Chem.* **1977**, *84*, 1-20.
5. Regis, A.; Corset, J. *Chem. Phys. Lett.* **1980**, *70*, 305-308.
6. Bunding, K. A.; Bell, M. I.; Durst, R. A. *Chem. Phys. Lett.* **1982**, *89*, 54-58.
7. (a) Tnaford, C. *The Hydrophobic Effect: Formation of Micelles and Biological Membranes*, 2nd Ed.; John Wiley & Sons: New York, 1980. (b) Fendler, J. H. *Membrane-Mimetic Approach to Advanced Materials*; Springer-Verlag: Berlin, 1994.
8. Voutsas, E. C.; Flores, M. V.; Spiliotis, N.; Bell, G.; Halling, P. J.; Tassios, D. P. *Ind. Eng. Chem. Res.* **2001**, *40*, 2362-2366.
9. Jang, N, H, M. *Ed. Thesis*, Seoul National University: Seoul, Korea, 1988.
10. Chung, M. I.; Tak, I. J.; Lee, K. M. *J. Korean Chem. Soc.* **1975**, *19*, 398-402.
11. (a) Youn, Y. W.; Lee, K. M. *J. Korean Chem. Soc.* **1975**, *19*, 289-293. (b) Lee, K. M. *J. Korean Chem. Soc.* **1976**, *20*, 193-197.
12. Lee, K. M. *J. Korean Chem. Soc.* **1973**, *17*, 73-79.
13. (a) Lee, Y. S.; Woo, K. W. *Bull. Korean Chem. Soc.* **1993**, *14*, 392-398. (b) Lee, Y. S.; Woo, K. W. *Bull. Korean Chem. Soc.* **1993**, *14*, 599-602. (c) Lee, Y. S.; Woo, K. W. *J. Colloid Interface Sci.* **1995**, *169*, 34-38.
14. Jang, N. H. *Bull. Korean Chem. Soc.* **2002**, *23*, 1790-1800.
15. Varsanyi, G. *Assignments for Vibrational Spectra of Seven Hundred Benzene Derivatives*; John Wiley & Sons: New York, 1974, and reference therein.
16. Lin-Vien, D.; Colthup, N. B.; Fately, W. G.; Grasselli, J. G. *The Handbook of Infrared and Raman Characteristic Frequencies of Organic Molecules*; Academic Press: London, 1991, and reference therein.
17. Brolo, A. G.; Irish, D. E.; Lipkowski, J. *J. Phys. Chem. B* **1997**, *101*, 3906-3909.
18. Simončič, B.; Špan, J. *Acta Chim. Slov.* **1998**, *45*, 143-152.